Articles

Contribution from the Department of Chemistry and Materials Science Center,
Cornell University, Ithaca, New York 14853-1301

Metal–Metal Interactions, a Pairing Distortion, and S-Lined Channels in the $M_2Ta_9S_6$ Structure

Maria José Calhorda[†] and Roald Hoffmann*

The ternary sulfides $M_2Ta_9S_6$ (M = Fe, Co, Ni) exhibit an interesting three-dimensional intermetallic structure, which also contains one-dimensional parallel channels sheathed by sulfur atoms. In the Ni derivative, all of the Ni atoms are equally spaced. On the other hand, a distortion occurs for the Fe and Co compounds, its main effect being a pairing of the 3d metals, which move out of their respective layers. Alternating M–M···M distances are observed. We used extended Hückel tight-binding calculations to study the bonding in these solids. Although the pairing distortion affects bands that might eventually lead to M–M bonds, we could detect little sign of their formation. We also probed the introduction of atoms in the hexagonal sulfur channels. Although the channels are very wide, strong bonds are formed between a large atom in the center and the three nearest sulfur atoms, in a triangular geometry around it.

The metal-rich sulfides $M_2Ta_9S_6$ (M = Co, Fe, Ni)[1,2] present us with a very interesting three-dimensional intermetallic structure containing one-dimensional channels sheathed by sulfur atoms. A comparable structure is also observed for the selenides $M_2Ta_{11}Se_8$ (M = Co, Fe, Ni),[3] where the selenium channels differ in size and geometry. The bulk of the $M_2Ta_9S_6$ structure consists of tantalum trigonal prisms, with M in the center and capping tantalum atoms in the rectangular faces. These units are stacked, are parallel to the channels, and are linked together by the capping tantalum atoms and sulfur atoms. This arrangement is interesting in that it differs markedly from that found in other tantalum sulfides. As a matter of fact, not only for the binary sulfides Ta_6S[4] and Ta_2S[5] but also for the early-transition-metal derivatives $M_xTa_{6-x}S$ (M = V, Cr; $x \approx 1$)[6] analogous columns consist of face-sharing pentagonal antiprisms or interpenetrating distorted icosahedra. These are connected by sulfur atoms, but channels are only observed in the structure of Ta_2S. The situation changes drastically when moving toward less metal-rich sulfides, as different structures are found. For instance, Ta_2NiS_5[7] and Ta_2NiSe_7[7b,8] are layered compounds, and the coordination around both Ta and Ni has changed.

Another striking characteristic of the ternary sulfide $M_2Ta_9S_6$ structure is the different behavior exhibited by nickel on the one hand and cobalt and iron on the other. $Ni_2Ta_9S_6$ is more symmetric with metal chains having equally spaced nickel atoms (3.37 Å apart). In cobalt and iron derivatives some pairing occurs and two different alternating M–M distances are found (they are respectively 2.88 and 3.70 Å for iron and 2.90 and 3.67 Å for Co), along with some distortion in the tantalum trigonal prisms.

In the present study, we shall try to understand the bonding in these solids and the reasons that lead to the observed distortions in some of them. The possible introduction of other atoms in the channels and their interaction with the sulfur atoms will also be examined.

The calculations used are of the extended Hückel type,[9] using the tight-binding method.[10] Details are given in the Appendix.

Structure of $Ni_2Ta_9S_6$

This compound crystallizes in the hexagonal space group $P\bar{6}2m$. A projection on the hexagonal plane of the atoms in a few unit cells is shown in Figure 1 (there is one formula unit per unit cell), revealing clearly the existence of empty spaces, which form the

channels running along c. Only sulfur atoms sheathe these channels.

Let us consider one of the nickel atoms (the two are in the $z = 0$ plane in the unit cell), which has as first neighbors six tantalum atoms in a trigonal prismatic coordination, **1**. A chain is built
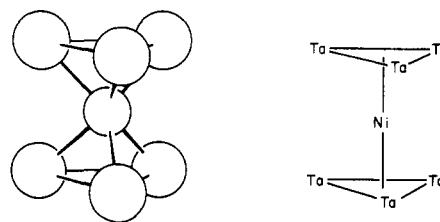
1

by repeating the $NiTa_3$ unit. Next, we add three other tantalum atoms, capping the prism rectangular faces ($z = 0$), as shown in **2**. Only sulfurs are now missing. They are bonded to tantalums
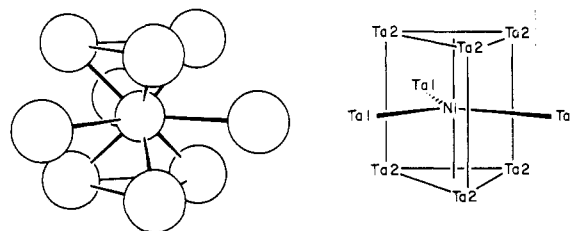

2

(1) Harbrecht, B.; Franzen, H. F. *J. Less-Common Met.* **1986**, *115*, 177.
(2) Harbrecht, B. *J. Less-Common Met.* **1986**, *124*, 125.
(3) Harbrecht, B. *J. Less-Common Met.*, in press.
(4) (a) Franzen, H. F.; Smeggil, J. G. *Acta Crystallogr.* **1970**, *B26*, 125. (b) Harbrecht, B. *J. Less-Common Met.* **1988**, *138*, 225.
(5) Franzen, H. F.; Smeggil, J. G. *Acta Crystallogr.* **1969**, *B25*, 1736.
(6) (a) Harbrecht, B.; Franzen, H. F. *Z. Krystallogr.* **1985**, *170*, 61. (b) Harbrecht, B.; Franzen, H. F. *Z. Anorg. Allg. Chem.* **1987**, *551*, 74.
(7) (a) Sunshine, S. A.; Ibers, J. A. *Inorg. Chem.* **1985**, *24*, 3611. (b) Sunshine, S. A.; Keszler, D. A.; Ibers, J. A. *Acc. Chem. Res.* **1987**, *20*, 395.
(8) Sunshine, S. A.; Ibers, J. A. *Inorg. Chem.* **1986**, *25*, 4355.
(9) (a) Hoffmann, R. *J. Chem. Phys.* **1963**, *39*, 1397. (b) Hoffmann, R.; Lipscomb, W. N. *J. Chem. Phys.* **1962**, *36*, 2179, 3489; **1962**, *37*, 2872.
(10) (a) Whangbo, M.-H.; Hoffmann, R. *J. Am. Chem. Soc.* **1978**, *100*, 6093. (b) Whangbo, M.-H.; Hoffmann, R.; Woodward, R. B. *Proc. R. Soc. London* **1979**, *A366*, 23.

[†] Permanent address: Centro de Química Estrutural, Instituto Superior Técnico, 1096 Lisbon Codex, Portugal.

as shown in **3**, for planes $z = 0$ and $z = c/2$, respectively. These


3
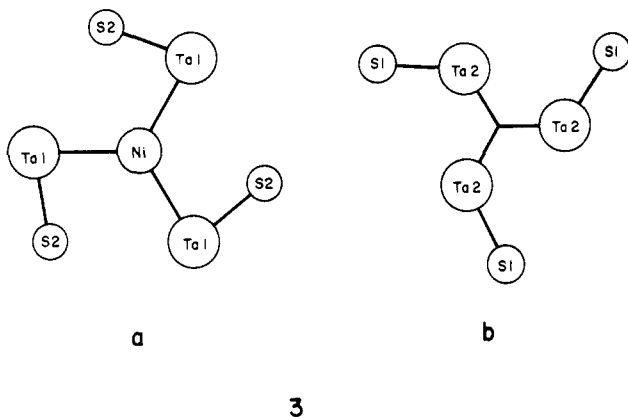
3-fold spiral motifs are like the coat of arms of the Isle of Man. They occur in "clockwise" and "counterclockwise" versions.

Chains along z are built by stacking alternately these two motifs. To get the three-dimensional structure we must see how these chains are horizontally linked by means of shared tantalum atoms (all the capping ones) and sulfur atoms, **4** (shared atoms are
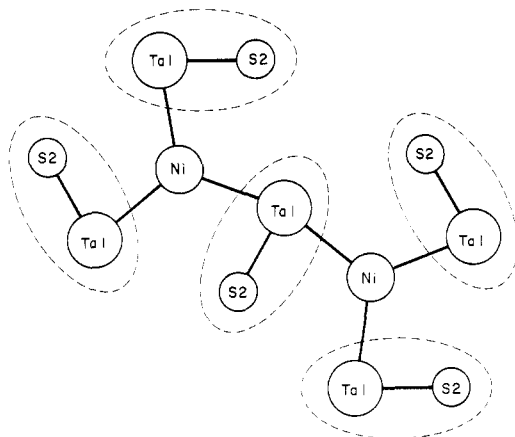

4a
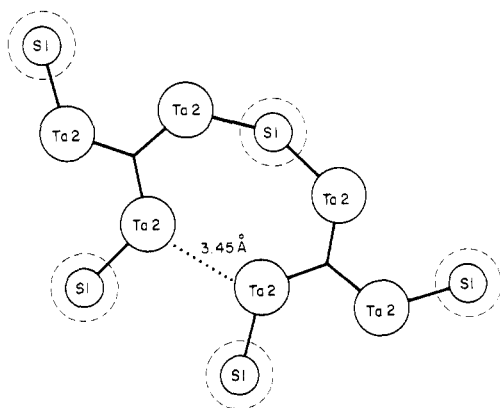
4b

enclosed in dashed-line circles). It should now be easy to look again at Figure 1 and understand how the different types of atoms are connected in the whole structure. Notice that the capping tantalums (Ta1) are not equivalent to those on the prism (Ta2); the same is happening to the sulfurs: S2 are bonded to Ta1, S1 to Ta2 (to use the same numbering system as in the original papers[1,2]), with different Ta–S bond lengths and Ta–Ta–S bond angles. Clockwise and counterclockwise Isle of Man motifs alternate as one moves from one stack to the adjoining one, meshing to form this beautiful structure.

Notice also that in the layer shown in **4b** ($z = c/2$) a relatively short Ta–Ta distance (3.45 Å) between two tantalum atoms in
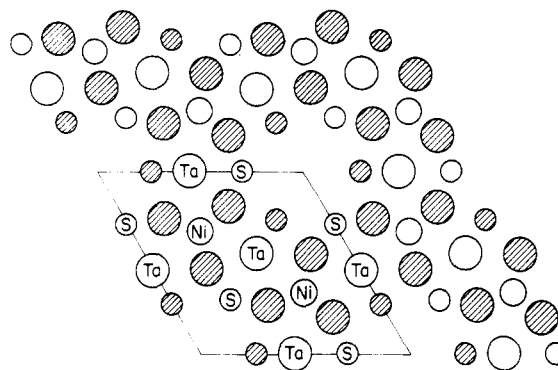

Figure 1. Structure of $Ni_2Ta_9S_6$ viewed along z. The larger circles are tantalum atoms, the medium ones nickel atoms, and the smaller ones sulfur atoms. The open circles are in the layer at $z = 0.0$, while the shaded circles belong to the layer at $z = 1.685$ Å. The hexagonal unit cell is outlined.

different triangles emerges. It is only a little bit longer than the Ta2–Ta2 distance between layers (3.37 Å), although much longer than the Ta2–Ta2 bond length in the triangles (3.19 Å).

Structure of $M_2Ta_9S_6$ (M = Co, Fe)

When the nickel atoms are replaced by cobalt or iron atoms, the following changes take place, **5**.
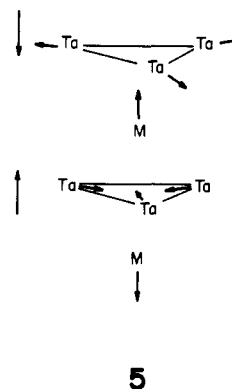
5

(1) The 3d transition metal is pushed away from the Ta1 plane, in the opposite direction each time, to form an alternation of longer and shorter metal–metal distances; they will be 3.67 and 2.90 Å for Co and 3.70 and 2.88 Å for Fe, respectively.

(2) The Ta2 triangle that is now closer to Co or Fe will expand; the other, farther away, will contract.

Although the unit cell is now doubled (along z) relative to that of $Ni_2Ta_9S_6$, the new c value is slightly (0.16 or 0.15 Å) smaller than twice the old one, meaning that a kind of compression of the whole structure occurs.

Band Structure of $Ni_2Ta_9S_6$

Most of the atoms in this structure have high coordination numbers. Nickel has six nearest tantalum neighbors (Ta2) at 2.49 Å and three others (Ta1) at 2.96 Å (**2**); each Ta2 is bonded to two other Ta2 atoms in the triangle (3.19 Å), two nickels, four Ta1 atoms (two above, two below) at 3.05 Å, one S1 atom (2.39 Å) and two S2 atoms (2.50 Å); Ta1 atoms have eight Ta2 neighbors, one S2 neighbor (2.545 Å), two S1 neighbors (2.52 Å), and two nickel neighbors. Let us add, for comparison, that the Ta metallic radius is 1.46 Å and the Ni radius is 1.24 Å.[11] This means that many Ta–Ta bonds are present, while a Ni–Ni distance of 3.37 Å is certainly too long for any direct interaction to be present.

Coordination numbers are smaller for the sulfur atoms. S1 atoms have two Ta2 atoms at 2.39 Å and two Ta1 atoms at 2.52 Å; S2 atoms have one Ta1 atom at 2.56 Å and four Ta2 atoms at 2.50 Å. Notice that if we consider one sulfur lying in a plane, its coordination sphere is all on one side of that plane; on the other side, there are no atoms. The shortest S–S distance is 3.32 Å: there are no S–S bonds. Four and five coordination of sulfur is

(11) Greenwood, N. N.; Earnshaw, A. *Chemistry of the Elements*; Pergamon Press: Oxford, England, 1984.
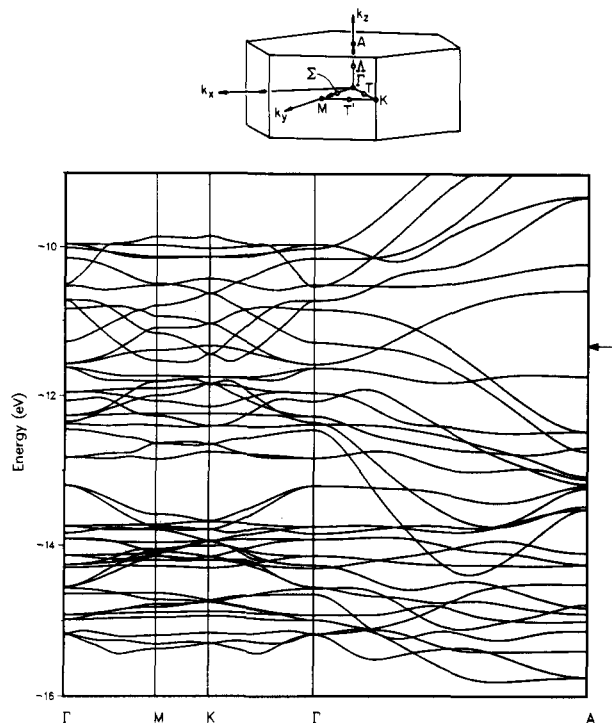
Figure 2. Brillouin zone for the hexagonal structure and the bands of $Ni_2Ta_9S_6$ plotted along several of its symmetry lines as indicated, in an energy window including the Fermi level.

Table I. Overlap Populations in $Ni_2Ta_9S_6$

	overlap pop.		
bond (d, Å)	layer 1 (3D)	layer 2 (3D)	complete structure
Ni–Ta1 (2.96)	0.244		0.061
Ta1–S2 (2.54)	0.681		0.400
Ni–Ni	0.000		0.000
Ni–Ni[a] (3.37)	0.074		−0.056
Ta2–Ta2 (3.19)		0.394	0.261
Ta2–Ta2[b] (3.45)		0.285	0.029
Ta2–S1 (2.39)		0.959	0.650
Ni–Ta2 (2.49)			0.234

[a] Nickel atoms in nearest layers of the same type. [b] Tantalums in adjacent chains.

are few sulfur states in the energy range −11 to −12 eV, where the Fermi level lies.

To try to understand what is happening, we looked separately at calculations of the two sets of sublattices from which the structure is built. Each sublattice is three-dimensional, but consists of only one type of layer.

The first one (layer at $z = 0$ in Figure 1) contains Ni, Ta1, and S2, as shown in the two-dimensional unit cell **6**. The Ta1

6

not unusual; that all the coordinating atoms are on one side of a plane is remarkable for the five-coordinate case. We will return to this later.

The presence of so many short bonds around each metal leads us to expect no simple, localized, crystal-field splitting of the d orbitals. Also, it is difficult to assign formal oxidation states to nickel and tantalum atoms. Assuming that sulfur is S^{2-}, sulfide, we must distribute 12 formal plus charges over 2 nickels and 9 tantalums. This is a true intermetallic compound.

Let us consider the Brillouin zone of the hexagonal lattice. We plotted the bands of the crystal along the symmetry lines $\Gamma \rightarrow M$, $M \rightarrow K$, $K \rightarrow \Gamma$ (in the central horizontal plane) and $\Gamma \rightarrow A$ (perpendicular direction, along z), as shown in Figure 2. The unit cell was wide and flat ($a = 10.134$ Å; $c = 3.37$ Å), so the opposite will hold in reciprocal space ($\Gamma \rightarrow A$ will be the longest line).

Only part of the bands are shown in the energy window. Their dispersion is much larger along $\Gamma \rightarrow A$ (corresponding to the channels and chains of the structure) than in the perpendicular plane, $\Gamma \rightarrow M \rightarrow K \rightarrow \Gamma$, where some gaps occur. A large gap (except along $\Gamma \rightarrow A$) is observed at ~ -13 eV and a narrower one at ~ -11.7 eV, not much below the Fermi level.

Among the bands exhibiting the largest dispersions along the symmetry line $\Gamma \rightarrow A$, four of them have strong contributions from the Ni z^2 orbital and two are crossed by the Fermi level (they are partially occupied). One might anticipate some distortion along z that would cause (after cell doubling and folding back the bands as described before[12,13]) gaps to open and a stabilization to occur for some specific electron counts. These would probably be lower than in the molecules studied here, as the bands appear to be more than half-filled.

We show in Figure 3 the total density of state (DOS) curve,[12] as well as the contributions of Ni 3d and Ta2 5d orbitals to that DOS. The dispersions of the d bands are large, but much more so for tantalum than for nickel. Although they are not shown here, the patterns of the projected densities of states for the other atoms, Ta1 and sulfurs, follow the same trends. However, there

5 d states spread over a large energy range, as do the sulfur ones, although not so much as in the whole three-dimensional structure. The total density of states (Figure 4) reveals the presence of gaps. Also, we see from the projected Ni 3d states, that 85% of them lie between −13 and −14.5 eV (the 3d orbital energy was taken as −13.49 eV), indicating a very small dispersion. This is not surprising, as the Ni–Ta1 distance is relatively long (2.96 Å). The interaction with the atoms in the neighboring layers will cause the dispersion observed in Figure 3 (many states were pushed down; others were pushed up).

In the other sublattice, the unit cell of which is shown in **7**, the

7

distances between atoms in each layer are shorter. A large dispersion of the Ta2 5d band is observed, due to Ta–S and Ta–Ta interactions.

We may compare some overlap populations, both in the layers and in the composite structure, to gain some feeling about the strength of the different interactions inside and between the layers.

(12) Hoffmann, R. *Angew. Chem.* **1987**, *99*, 871; *Angew Chem., Int. Ed. Engl.* **1987**, *26*, 846.

(13) Whangbo, M.-H. In *Crystal Chemistry and Properties of Materials with Quasi-One-Dimensional Structures*; Rouxel, J., Ed.; Reidel: Dordrecht, The Netherlands, 1986.
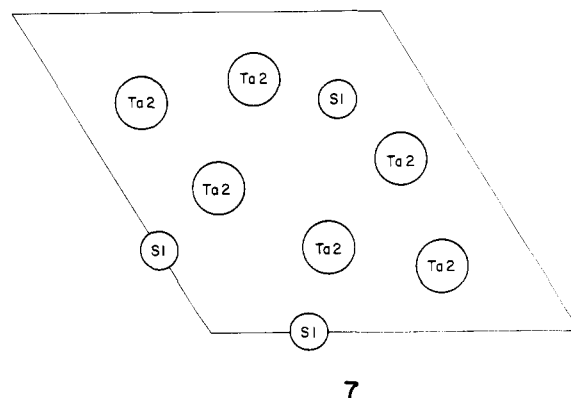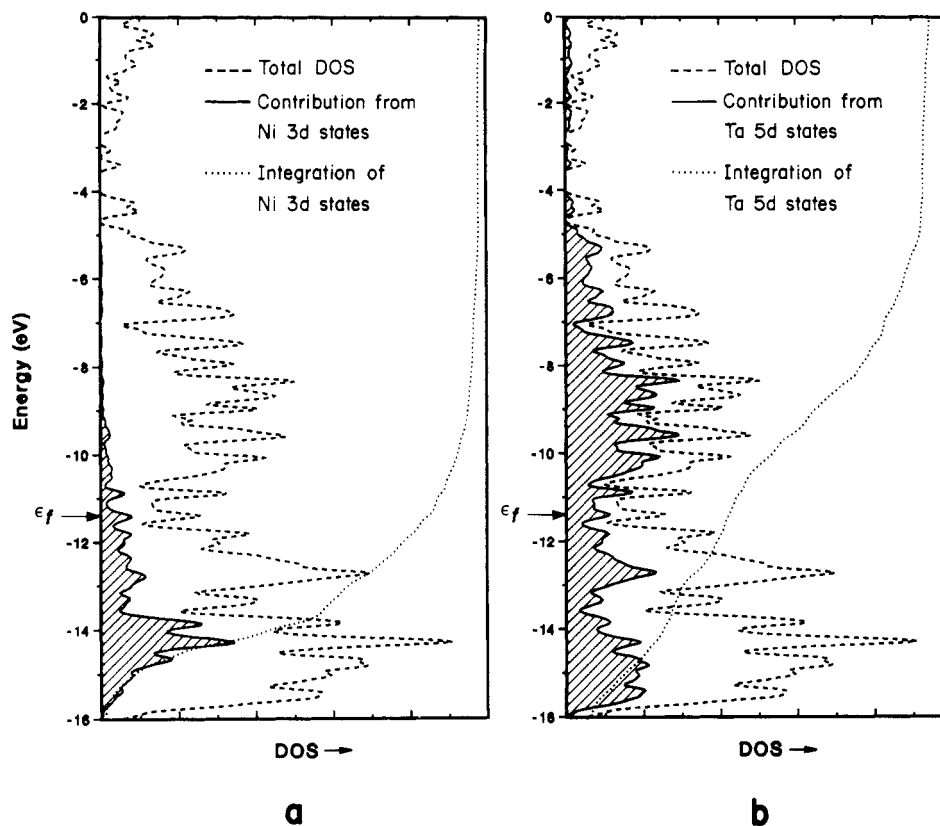
Figure 3. Total density of states (DOS) for the $Ni_2Ta_9S_6$ structure (--), the projection of d states (—) for Ni 3d (a) and Ta 5d (b), and their respective integrations (⋯).
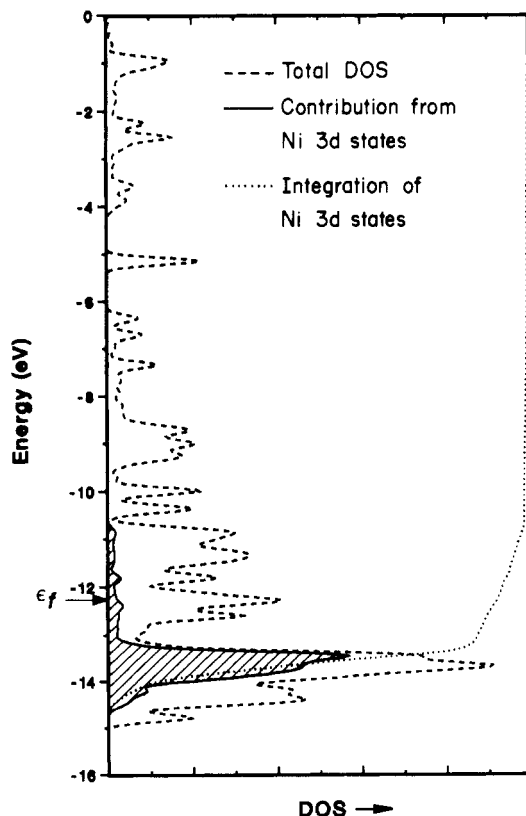
Figure 4. Total density of states (DOS) for a sublattice containing Ni, Ta1, and S2, as shown in **6** (---) and a projection (—) and integration (⋯) of the Ni 3d states.

These are collected in Table I. Some care must be taken in using these figures, but some conclusions are straightforward. Aside from the Ta–S bonds, the Ta2–Ni and Ta2–Ta2 (in the triangle) bonds are the strongest. On the other hand, the Ni–Ni overlap

population is almost zero. These are the bonds that are more markedly affected by the distortion observed when nickel is replaced by cobalt or iron. Bonds between tantalum atoms in different layers, Ta1 and Ta2, are also formed (the overlap populations are 0.193 and 0.167 for the two kinds of bonds).

While the electronic structures of the two layers making up the $Ni_2Ta_9S_6$ structure are instructive in and of themselves, they really do not help us understand the parent structure. For instance the large differences in Ni–Ta, Ta–Ta, and Ta–S overlap populations between the layers and the whole molecule, point to the obvious—interlayer interactions are critical. Other attempts at carving out substructures of lower dimensionality, e.g. one-dimensional $NiTa_3$, $NiTa_3S_3$, NiTa, and $NiTa_6S_6$ based on **2**, were also not informative. These are complex intermetallic compounds, with all elements involved in a three-dimensional bonding network.

Metal–Metal Pairing Distortion

A possible approach to analyzing the distortion would be to allow the Ni atoms to move away from the layer they belong to, as the first step, and then to contract and expand the Ta2 triangles. This implies a doubling of the unit cell along z (the direction in which changes occur).

Let us consider the first step only. As this particular distortion takes place, the nickel–nickel bond lengths (along z) will alternate between 2.95 and 3.79 Å (compared to a uniform 3.37 Å distance before distortion). We made calculations for different electron counts, corresponding to Ni, Co, and Fe $M_4Ta_{18}S_{12}$ species, but keeping the Ni parameters. The energy per unit cell does not change much ($\Delta \sim 0.03$ eV; Δ positive means the distorted structure is at lower energy) for Ni and decreased by 0.18 and 0.55 eV for Co and Fe, respectively (i.e. Δ grew more positive). These changes are too small to be trusted, although they mimic the experimental data. However, the initial Ni–Ni overlap population of –0.056 is not significantly altered (to ~–0.04 for the "short" bond and ~–0.06 for the long one). As there is not much to be gained by observing these results, we move to the next step of the distortion, which is going to affect the Ta2 atoms (all the others, Ta1 and sulfurs, remain approximately in the same positions). The new results are collected in Table II and include

Table II. Energy/Unit Cell, Fermi Energy, and Overlap Populations for $M_2Ta_9S_6$ (Fe, Co, and Ni Electron Counts)[a]

	M = Ni		M = Co		M = Fe	
	A	B	A	B	A	B
energy, eV	-3050.55	-3051.17	-3004.47	-3005.44	-2957.21	-2958.84
Fermi level, eV	-11.32	-11.28	-11.74	-11.57	-11.94	-11.87
overlap pop.						
M–M	-0.056	-0.058	-0.055	-0.057	-0.055	-0.053
		-0.038		-0.038		-0.036
M–Ta2	0.234	0.281	0.250	0.296	0.258	0.311
		0.198		0.207		0.212
Ta2–Ta2	0.261	0.185	0.248	0.182	0.246	0.177
		0.352		0.345		0.341

[a] A = undistorted structure; B = distorted structure.


a   **b**   **c**
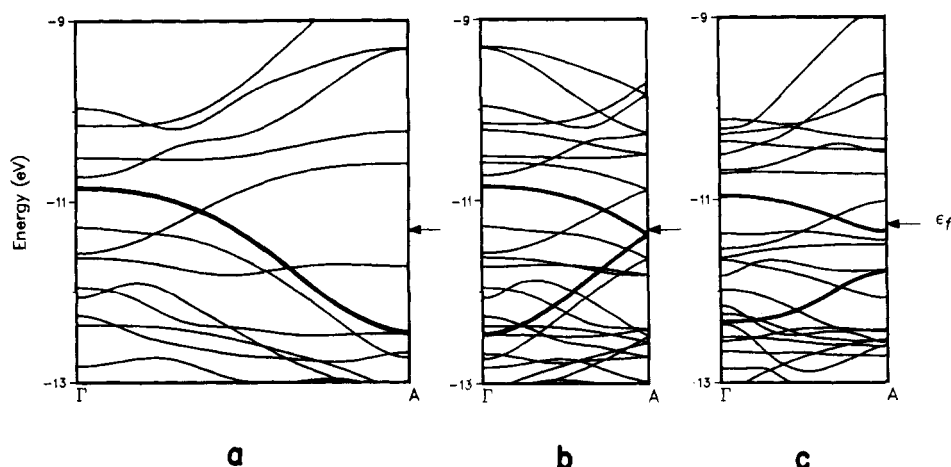
Figure 5. Bands of $M_2Ta_9S_6$ along the symmetry line $\Gamma \rightarrow A$ of the Brillouin zone, in the energy range around the Fermi level: (a) for the undistorted $M_2Ta_9S_6$; (b) for the same $M_2Ta_9S_6$ structure, but using a unit cell that was doubled; (c) for the distorted $M_2Ta_9S_6$.

energy/unit cell, Fermi level, and some overlap populations.

The tendency toward distortion has increased in the series, as the energy is lowered by 0.62 eV for Ni, 0.97 eV for Co, and 1.63 eV for Fe. Once again the trend is correct, in that the Co and Fe structures are more stabilized by distortion. The calculation is not correct in indicating that the Ni structure should also undergo the pairing distortion, which to our knowledge does not occur.

Once again, there is almost no change in the M–M overlap population, which is very small and negative. To have some feeling about what a Ni–Ni overlap population could be, some calculations were made for one of the complexes considered to have a full Ni–Ni single bond, $Ni_2(CN)_6^{4-}$.[14] The structure has been determined for the Rb^+ [15] and K^+ [16] salts. Each nickel atom has a square-planar coordination to three cyanide ligands and the other nickel, the two $Ni(CN)_3$ units being in almost perpendicular planes, with a Ni–Ni bond length of ca. 2.30 Å, **8**. The overlap
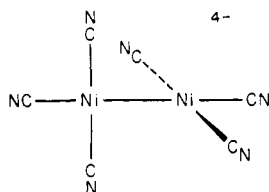
8

population for the Ni–Ni bond in this dimeric complex was calculated to be 0.26 at the experimental bond length, 0.27 for d(Ni–Ni) = 2.90 Å, and 0.24 for d(Ni–Ni) = 3.50 Å. Even allowing for the fact that extended Hückel calculations are not very reliable in dealing with changes in distances, the order of magnitudes are so different for the Ni–Ni overlap populations

in the dimer and in $Ni_2Ta_9S_6$ that it seems safe to conclude that there are no Ni–Ni bonds in the latter, both in the undistorted and distorted forms. The driving force for the distortion has then to be looked for somewhere else.

We only listed in Table II overlap populations that changed considerably as a result of the distortion, which are the Ni–Ta2 and Ta2–Ta2 (inside the triangles) overlap populations. There are now two types of Ta2 atoms, those in the expanded and those in the contracted triangles (**5**), and two types of M–Ta2 (2.41 and 2.57 Å) and Ta2–Ta2 (3.31 and 3.01 Å) bonds, for which two sets of overlap populations are given in Table II. For some other bonds, a shortening of the bond length was not accompanied by an increase of overlap population. One example is the Ta2–Ta2 bond between adjacent triangles. This was a strong bond in layer 2 (see Table I). However, as Ta2–Ni bonding is switched on, it becomes weaker and approaching the two atoms does not help very much (overlap population is only 0.070 for the distorted nickel derivative). Changes in Ta1 to Ta2 overlap populations parallel the changes in the respective bond lengths.

Let us look at the band structure to see if we can get some more information about the levels involved in the distortion. We saw in Figure 2 the bands of the undistorted $Ni_2Ta_9S_6$. The dispersion was small in the hexagonal plane of the Brillouin zone and large along the perpendicular. As this is the direction where changes are more likely to occur (due to "pairing" of Ni atoms and alternating Ni–Ta2 bond lengths), we shall concentrate on it. However, the unit cell of the distorted structure is doubled along c, the Brillouin zone will be halved, and the bands are folded back. We show in Figure 5a the bands along $\Gamma \rightarrow A$ in the $Ni_2Ta_9S_6$ structure in the energy range around the Fermi level. In Figure 5b we have an equivalent representation, only the bands are folded back, due to doubling the unit cell. In Figure 5c, we see the bands corresponding to a structure distorted as $Fe_2Ta_9S_6$. Some gaps are opened across the line $\Gamma \rightarrow A$ as a consequence of the distortion. Many bands become flatter, some are stabilized, and others are destabilized.

It would be extremely helpful to have a simple model that would allow us to look for an interpretation of what is occurring in our

(14) Summerville, R. H.; Hoffmann, R. *J. Am. Chem. Soc.* **1976**, *98*, 7240.
(15) Jarchow, O. *Z. Anorg. Allg. Chem.* **1971**, *383*, 40.
(16) Jarchow, O.; Schulz, H.; Nast, R. *Angew Chem., Int. Ed. Engl.* **1970**, *9*, 71.

complicated structure. We studied three different linear chains of increasing complexity. The first, simpler, model was a chain built from stacking $NiTa_3$ units as in **1**. In the second one, the three capping tantalums were added, and the chain consisted of $NiTa_6$ units linked as shown in **2**. The third model chain was obtained by stacking alternately the two units represented in **3**. A major problem in these models is that while the nickel atoms are well modeled, the same cannot be said for the tantalums. Their coordination numbers are smaller. Another difficulty arises from the uncertainty about formal oxidation states.

As a consequence, the results of the calculations showed no agreement between the energetics of the same distortions in any of these model chains and in the real structure. For instance, the tendency to distort did not appear to increase with decreasing electron count, as it should. On the other hand, some features remained, such as the absence of positive overlap populations for the Ni–Ni bonds. The same trends were observed for Ni–Ta and Ta–Ta overlap populations as in the complete structure.

Let us go back to a more detailed look at the bands in Figure 5. We can consider the band drawn broader in Figure 5a and see how it is affected by the distortion. This band is broad and is cut by the Fermi level. At Γ, this band has contributions from Ni z^2 (the nickel orbitals in the unit cell are in phase), Ta2 (an orbital that resembles z^2 but is a mixture of orbitals, due to the general positions of Ta2 in the structure), and other atoms. A representation is shown in **9**, considering only one of the nickel atoms and its Ta2 neighbors in the unit cell.

9
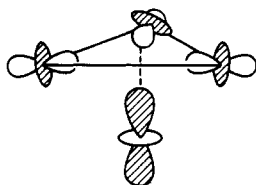
Along Γ to A in the Brillouin zone the z bands will have the same type of symmetry as the z^2 bands and can mix. As a result, at A, the Ni contribution to the band will be z (a simplified representation is given in **10**). The way the band runs along the
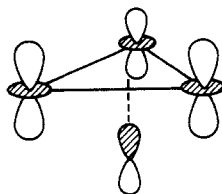
10

zone is difficult to predict as so many orbitals are involved (not only those shown in **9** and **10**).

After the distortion takes place, symmetry is lost and with it the degeneracies observed at point A for the double unit cell. A large gap is opened. The upper half of the band is only slightly destabilized in most of the zone. If this were the only band to be affected by the distortion, the distortion should be favorable even for nickel (it is little more than half-filled) and even more for less electron-rich Co and Fe. Also, this band is strongly Ta2–Ta2 bonding and Ni–Ta2 antibonding, as can be confirmed for the upper half by the crystal orbital overlap population (CO-OP) curve (there are only a few bands between -11.0 and -11.3 eV), but not for the lower part (it lies in a crowded region).

The band that comes next (at lower energy) in Figure 5a also has some Ni z^2 character at Γ, and the Ni orbitals are out of phase in the unit cell. It runs almost parallel to the other band we examined and will be similarly affected by the distortion. Its upper half still lies next to our initial band, at Γ, in Figure 5c, and is also destabilized by the distortion. It is completely filled in the
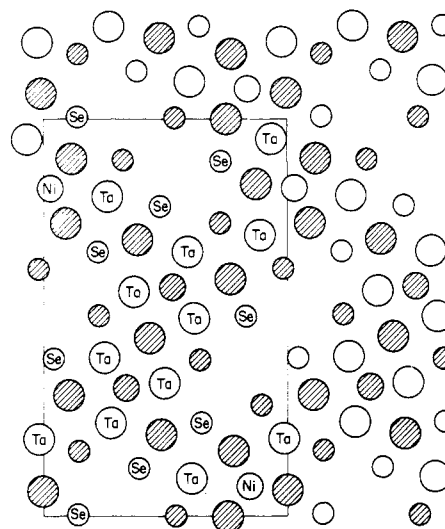
Figure 6. Structure of $M_2Ta_{11}Se_8$ viewed along z, showing the rectangular channels sheathed by Se atoms. The larger circles are tantalum atoms, the medium ones nickel atoms, and the smaller ones selenium atoms. The open circles are in the layer at $z = 0.0$, while the shaded circles belong to the layer at $z = c/2$.

Ni derivative but probably only partially for Co and Fe.

At this point it might seem that the deformation observed is a simple pairing distortion, driven by metal–metal bonding. The lower part of each "z^2" band is M–M bonding; the upper part is M–M antibonding. The lower parts are filled and the upper part is partially so. However, we are hesitant to draw this conclusion. First, these bands that we have singled out for analysis have substantial Ta character and are not very localized on Ni. Second, the enhanced M–M bonding that should follow the distortion just does not show up in the diagnostic overlap populations.

It is interesting to consider the group of related species $M_2Ta_{11}Se_8$ (M = Fe, Co, Ni).[3] In the Ni derivative, this metal is surrounded by tantalum atoms in much the same way as in $Ni_2Ta_9S_6$ (Ta2 trigonal prisms, Ta1 capping its faces). What is different now is the way the basic chains are linked together to form the three-dimensional structure. This is not simply layered as in the compounds studied in this paper. Adjacent chains are displaced relative to one another by half the repeat distance along c. Also, the channels, now sheathed by selenium atoms, are rectangular, not hexagonal (horizontal section of the structure), as can be seen in Figure 6.

When Ni is replaced by Co or Fe, some disorder is observed in their structures. There are some local distortions, but they are not periodically repeated along the structure. There is no pairing distortion.

Similar calculations on these $M_2Ta_9S_6$ systems have been carried out independently by T. Hughbanks.[17]

Sulfur Channels

We saw in Figure 1 the open channels running along c in the three-dimensional structure of $Ni_2Ta_9S_6$, which look hexagonal when viewed in that projection. Each channel is formed by six sulfurs from four adjacent unit cells. Three of them lie at $z = 0$ (S2, open small circles in Figure 1) and the other three at $z = c/2$ (S1, shaded small circles in Figure 1).

It is obvious that one should try to introduce other atoms in those channels, as that might lead to some interesting new materials. There are examples of such situations, one of them being observed for $Tl_xV_6S_8$.[18] Here thallium atoms are found in hexagonal channels, and the properties of the materials depend on the stoichiometry.

The two kinds of sulfur atoms have different coordination polyhedra. S1 occupies the apex of a distorted tetragonal pyramid,

(17) Hughbanks, T., private communication.
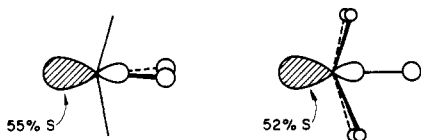(18) Schlögl, R.; Bensch, W. *J. Less-Common Met.* **1987**, *132*, 155.

**11**, while S2 is pentacoordinate, **12**.
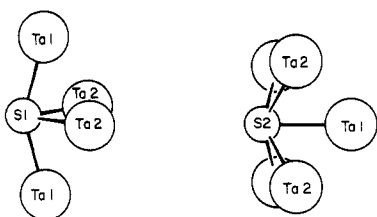
11   **12**

The geometry suggests a sulfur lone pair, pointing away from the ligands, for each geometry. For a model SH_4 or SH_5 fragment with the same geometry we find such a lone pair, for which the energy is -14.26 or -14.30 eV, respectively, **13**.

13

Three limiting geometries may be considered for an atom of M inside the channel: triangular coordination to S2, **14**, triangular coordination to S1, **15**, and distorted octahedral coordination to S2 and S1, **16**. The M-S bond lengths are quite large, especially M-S1.

d(M-S2)=2.99 Å   d(M-S1)=2.72 Å   d(M-S1)=2.85 Å
                                                 d(M-S2)=3.11 Å
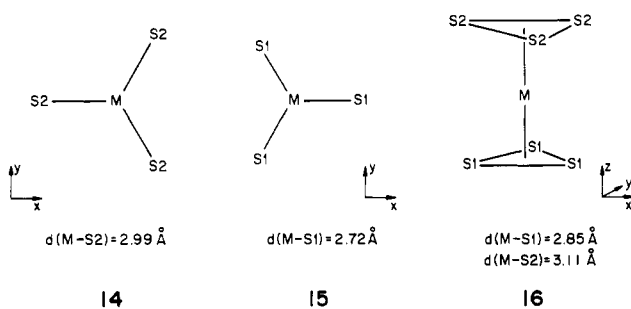
14   **15**   **16**
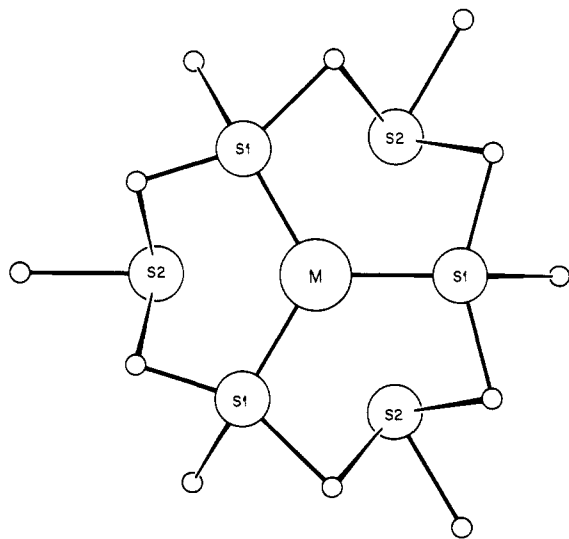
To probe the bonding in the sulfur channels, we built a simple model, keeping the sulfur atoms and replacing Ta1 and Ta2 by H, at the same distances (unit cell **17**). We then introduced Cu

17

and Au atoms in the channels, as in **14–16**. In Table III, some overlap populations are given, for a unit cell $MS_6H_{12}^+$, as well

Table III. Overlap Populations for Bonds in the Sulfur Channel Chains, $MS_6H_{12}^+$

	overlap pop.					
	M = Cu			M = Au		
	14	15	16	14	15	16
M–S1	0.030	0.193	0.130	0.048	0.268	0.188
M–S2	0.074	0.003	0.042	0.111	0.005	0.067
M–M	0.004	0.000	0.002	0.014	0.005	0.009
energy, eV	-886.56	-887.57	-887.07	-897.59	-898.70	-898.16

Table IV. Parameters Used in the Extended Hückel Calculations

atom	orbital	H_{ii}/eV	ζ_1	ζ_2	$c_1{}^a$	$c_2{}^a$
Ni	4s	-9.17	1.83			
	4p	-5.15	1.12			
	3d	-13.49	5.75	2.00	0.5683	0.6292
Ta	6s	-10.10	2.28			
	6p	-6.86	2.24			
	5d	-12.10	4.76	1.938	0.6105	0.6105
S	3s	-20.00	1.82			
	3p	-13.30	1.82			

^{a}Coefficients used in the double-ζ expansion of the d orbitals.

as the energies. The preferred coordination geometry is **15**, triangular, with M linked to S1. The energy is lowest, and bonding is maximized. The overlap populations are larger for gold than for copper, as the long M-S distances are more compatible with a bigger atom.

The lone pairs of S1 will lie in the plane parallel to xy, at z = 1.685 Å. Their three linear combinations look (only the sulfur contributions) as in **18**.

E = -13.64 eV   E = -13.54 eV   E = -13.52 eV
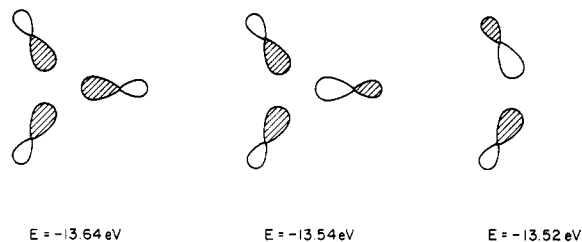
18

In the DOS of the composite $MS_6H_{12}^+$ polymer (M = Au, Cu), we found evidence for interaction of these lone pair combinations with M s and x,y orbitals. This is reflected in the M-S overlap populations in Table III.

Let us now consider a metal atom, gold, in a sulfur channel of the three-dimensional structure. If they are spaced as before (3.37 Å) there will be one gold per unit cell, $AuNi_2Ta_9S_6$. We studied only the more favorable coordination geometry, as found for the model. In the complete structure, each gold atom will be bound to three S1 atoms (at z = 1.685 Å), as in **15**. The overlap populations Au-S1 are now 0.227. They are of the same order of magnitude as in the model. Another indication of gold–sulfur interaction is given by the spreading of the gold bands, which are widely dispersed over the range between -16 and -3.5 eV. The net charge on the gold atom is +0.30.

One difficulty arising in this kind of comparison concerns the electron count. The sulfur lone pairs have energies much below the Fermi level, but they give rise to broad bands when the channels are assembled. However, in the calculations described, the net charges on the sulfur atoms were quite similar for both the model S_6H_{12} chain and the $Ni_2Ta_9S_6$ structure.

These results suggest that the sulfur channels may be occupied by other metal atoms, preferably large ones, due to the width of the cavity. This also favors three coordination to the three nearest sulfur atoms, instead of a distorted octahedral coordination. If smaller metal atoms are introduced, perhaps more than one per

formula unit could enter the channels. The introduction of this new atom in the structure did not open any gaps in the total density of states, and the new material should still be metallic.

Appendix

All of the calculations were of the extended Hückel type,[9] with

the tight-binding approach.[10] The parameters used are collected in Table IV.

The geometry of $Ni_2Ta_9S_6$[1,2] was used as the undistorted structure. In the study of distortion the same unit cell parameters a and $c' = 2c$ were taken, but the general positions of the atoms in $Fe_2Ta_9S_6$ were used.

The k-point sets were chosen according to the size of the unit cell, using the method of Ramirez and Böhm.[19]

Registry No. $Fe_2Ta_9S_6$, 101238-71-5; $Co_2Ta_9S_6$, 101238-67-9; Ni_2-Ta_9S_6, 101238-83-9; S, 7704-34-9.

(19) Ramirez, R.; Böhm, M. C. *Int. J. Quantum Chem.* **1986**, *30*, 391.

Contribution from the Laboratory of Organic Chemistry, Delft University of Technology, Julianalaan 136, 2628 BL Delft, The Netherlands

# Multinuclear NMR Study of Lanthanide(III) Complexes of Diethylenetriaminepentaacetate

Joop A. Peters

The complexation of lanthanide(III) cations with diethylenetriaminepentaacetate (DTPA) in the presence of lithium as counterion in aqueous solution has been investigated with the use of ^{13}C, ^{17}O, and ^6Li NMR shift and relaxation measurements. The data show that the DTPA ligand is bound octadentately via the three nitrogens and the five carboxylates. Conformational interconversions, taking place in the DTPA ligand, give rise to exchange broadening in the ^{13}C and ^1H NMR spectra. The first coordination sphere is completed by one water, while two lithium counterions are present in the second coordination sphere. The counterions are probably exchanging between the various carboxylate groups.

Introduction

The paramagnetic lanthanide(III) ions have a pronounced influence on the chemical shifts and relaxation rates of nuclei in their proximity.[1–3] The enhancement of longitudinal and transverse relaxation rates by, particularly, Gd^{III} has been successfully applied to improve contrast in magnetic resonance imaging. In order to reduce its toxicity, the Gd^{III} in contrast agents is bound by a very strong chelator such as diethylenetriaminepentaacetate (DTPA).[4,5]
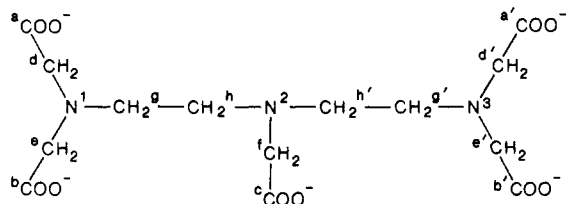
The X-ray crystal structure determinations of Na_2Gd-$(DTPA)\cdot H_2O$[6] and $BaNd(DTPA)\cdot 3H_2O$[7] revealed that in the solid

state the Ln^{III} cation is coordinated to the three nitrogens and five carboxylate oxygens of DTPA and to a water. Several studies of the coordination of DTPA by Ln^{III} cations have been reported. Both hepta-[8,9] and octadentate structures[10,11] have been proposed for the DTPA ligand, and it has been shown that in solution one water is coordinated to the Ln^{III} cation.[10,12,13]

This paper reports the results of a multinuclear NMR study on the structure of Ln^{III}–DTPA complexes in aqueous solution. Chemical shifts and Nd^{III}-induced ^{13}C relaxation rate enhancements were used to determine the denticity of the DTPA ligand and to obtain information on its structure, whereas Ln^{III}-induced ^{17}O water shifts were employed to determine the water coordination number. In order to get an impression about the location of the monovalent counterions near the negatively charged Ln^{III}–DTPA complex, ^6Li NMR techniques were applied.

Experimental Section

The $LnCl_3\cdot xH_2O$ salts were purchased from Alfa Products. The Ln^{III} content was determined by an EDTA titration using arsenazo I as the indicator. The DTPA used was obtained as the acid ($H_5(DTPA)$) from Fluka A.G. The solutions used in this study were prepared by dissolving $H_5(DTPA)$ in a solution of an equivalent amount of LiOH in D_2O. Then the Ln^{III} salt was added, and the pD was adjusted with DCl or LiOH in D_2O.

(1) Sherry, A. D.; Geraldes, C. F. G. C. In *Lanthanide Probes in Life, Medical, and Environmental Sciences: Theory and Practice*; Bünzli, J.-C., Choppin, G. R., Eds.; Elsevier: Amsterdam, 1988; Chapter 3.
(2) Inagaki, F.; Miyazawa, T. *Prog. Nucl. Magn. Reson. Spectrosc.* **1981**, *14*, 67.
(3) Peters, J. A.; Kieboom, A. P. G. *Recl. Trav. Chim. Pays-Bas* **1983**, *102*, 381.
(4) Laniado, M.; Weinmann, H. J.; Schörner, W.; Felix, R.; Speck, U. *Physiol. Chem. Phys. Med. NMR* **1984**, *16*, 157.
(5) Goldstein, E. J.; Burnett, K. R.; Hansell, J. R.; Casaia, J.; Dizon, J.; Farrar, B.; Gelblum, D.; Wolf, G. L. *Physiol. Chem. Phys. Med. NMR* **1984**, *16*, 97.
(6) Gries, H.; Miklautz, H. *Physiol. Chem. Phys. Med. NMR* **1984**, *16*, 105.

(7) Stezowski, J. J.; Hoard, J. L. *Isr. J. Chem.* **1984**, *24*, 323.
(8) Choppin, G. R.; Baisden, P. A.; Khan, S. A. *Inorg. Chem.* **1979**, *18*, 1330.
(9) Geraldes, C. F. G. C.; Sherry, A. D. *J. Magn. Reson.* **1986**, *66*, 274.
(10) Alsaadi, B. M.; Rossotti, F. J. C.; Williams, R. J. P. *J. Chem. Soc., Dalton Trans.* **1980**, 2151.
(11) Kostromina, N. A.; Ternovaya, T. V. *Russ. J. Inorg. Chem. (Engl. Transl.)* **1979**, *24*, 1024.
(12) Bryden, C. C.; Reilley, C. N. *Anal. Chem.* **1982**, *54*, 610.
(13) Koenig, S. H.; Baglin, C.; Brown, R. D., III; Brewer, C. F. *Magn. Reson. Med.* **1984**, *1*, 497.